Report

Current Biology

# A Convergent and Essential Interneuron Pathway for Mauthner-Cell-Mediated Escapes

## Graphical Abstract

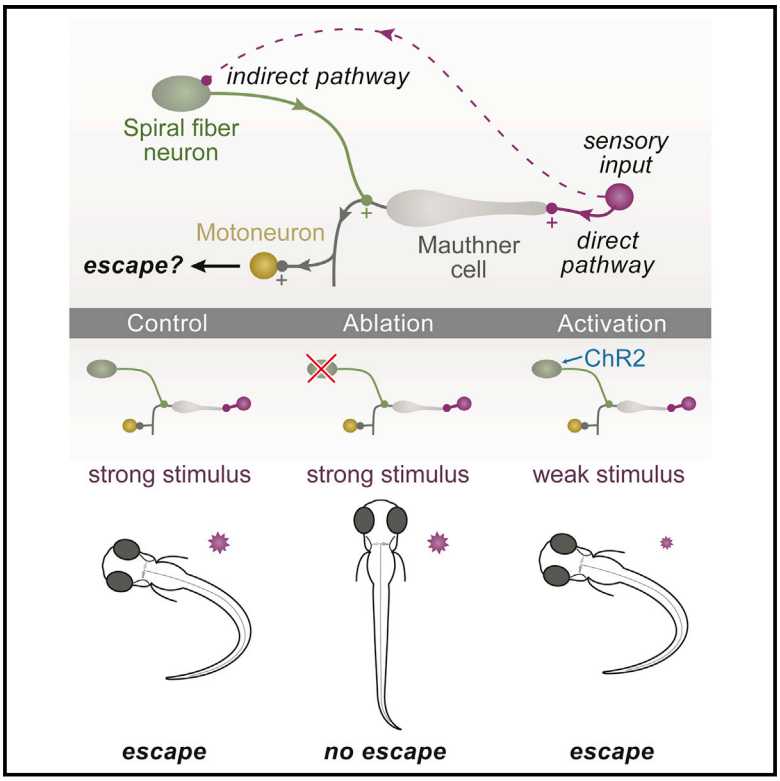


## Authors

Alix M.B. Lacoste, David Schoppik, ..., Florian Engert, Alexander F. Schier

## Correspondence

schier@fas.harvard.edu

## In Brief

Lacoste et al. find that excitatory interneurons form an essential feedforward pathway for the Mauthner-cell-mediated startle behavior of larval zebrafish. Together with direct sensory afferents on the lateral dendrites, the input of spiral fiber neurons at the axon hillock of the Mauthner cell enables fast escapes in response to noxious stimuli.

## Highlights

- Spiral fiber neurons excite Mauthner cells, which mediate fast escape behavior
- Calcium imaging reveals that spiral fiber neurons encode aversive sensory cues
- Ablation and optogenetic experiments indicate that they are essential for escapes
- This study uncovers the crucial role of a feedforward excitatory motif for behavior

Lacoste et al., 2015, Current Biology *25*, 1–9
June 1, 2015 
http://dx.doi.org/10.1016/j.cub.2015.04.025

CellPress

Please cite this article in press as: Lacoste et al., A Convergent and Essential Interneuron Pathway for Mauthner-Cell-Mediated Escapes, Current Biology (2015), http://dx.doi.org/10.1016/j.cub.2015.04.025

Current Biology
Report



# A Convergent and Essential Interneuron Pathway for Mauthner-Cell-Mediated Escapes

Alix M.B. Lacoste,[1] David Schoppik,[1,7] Drew N. Robson,[1,8] Martin Haesemeyer,[1] Ruben Portugues,[1,9] Jennifer M. Li,[1,8] Owen Randlett,[1] Caroline L. Wee,[2] Florian Engert,[1] and Alexander F. Schier[1,3,4,5,6,*]
[1]Department of Molecular and Cellular Biology, Harvard University, Cambridge, MA 02138, USA
[2]Program in Neuroscience, Harvard Medical School, Boston, MA 02115, USA
[3]Center for Brain Science, Harvard University, Cambridge, MA 02138, USA
[4]Broad Institute of MIT and Harvard, Cambridge, MA 02142, USA
[5]Harvard Stem Cell Institute, Cambridge, MA 02138, USA
[6]FAS Center for Systems Biology, Harvard University, MA 02138, USA
[7]Present address: Neuroscience Institute, New York University Langone School of Medicine, New York, NY 10016, USA
[8]Present address: Rowland Institute at Harvard, Cambridge, MA 02142, USA
[9]Present address: Max Planck Institute of Neurobiology, 82152 Martinsried, Germany
*Correspondence: schier@fas.harvard.edu
http://dx.doi.org/10.1016/j.cub.2015.04.025

## SUMMARY

**The Mauthner cell (M-cell) is a command-like neuron in teleost fish whose firing in response to aversive stimuli is correlated with short-latency escapes [1–3]. M-cells have been proposed as evolutionary ancestors of startle response neurons of the mammalian reticular formation [4], and studies of this circuit have uncovered important principles in neurobiology that generalize to more complex vertebrate models [3]. The main excitatory input was thought to originate from multisensory afferents synapsing directly onto the M-cell dendrites [3]. Here, we describe an additional, convergent pathway that is essential for the M-cell-mediated startle behavior in larval zebrafish. It is composed of excitatory interneurons called spiral fiber neurons, which project to the M-cell axon hillock. By in vivo calcium imaging, we found that spiral fiber neurons are active in response to aversive stimuli capable of eliciting escapes. Like M-cell ablations, bilateral ablations of spiral fiber neurons largely eliminate short-latency escapes. Unilateral spiral fiber neuron ablations shift the directionality of escapes and indicate that spiral fiber neurons excite the M-cell in a lateralized manner. Their optogenetic activation increases the probability of short-latency escapes, supporting the notion that spiral fiber neurons help activate M-cell-mediated startle behavior. These results reveal that spiral fiber neurons are essential for the function of the M-cell in response to sensory cues and suggest that convergent excitatory inputs that differ in their input location and timing ensure reliable activation of the M-cell, a feedforward excitatory motif that may extend to other neural circuits.**

## RESULTS

Activity in Mauthner cells (M-cells), a pair of large neurons located bilaterally in the hindbrain and projecting directly to motoneurons, is associated with escapes of short latencies [5–8]. Spiral fiber neurons are a group of neurons that project to the contralateral M-cell [9], where they wrap around the axon hillock at a structure called the axon cap [10]. Previous studies suggest that spiral fiber neurons excite the M-cell in adult goldfish [11], and stimulation of a single spiral fiber neuron in larval zebrafish is capable of eliciting an excitatory post-synaptic potential (EPSP) in the contralateral M-cell [9]. Anatomical [10], as well as electrophysiological and pharmacological [9], evidence points to the presence of both glutamatergic and electrical synapses between spiral fiber neurons and the M-cell. Based on these studies, spiral fiber neurons are well positioned to influence the M-cell-mediated escape behavior. In fact, mutants for the *retinoblastoma-1* gene that have defects in axon targeting, including in the spiral fiber neurons, display abnormal turning movements in response to touch [12, 13]. However, the stimuli that drive the spiral fiber neurons have yet to be identified and their role in the M-cell escape network remain unclear. Here, we address these questions using functional calcium imaging, ablations, optogenetics, and behavior analysis.

### Spiral Fiber Neurons Respond to Aversive Stimuli

We used a transgenic line, *Tg(–6.7FRhcrtR:gal4VP16)*, that labels spiral fiber neurons and other neurons in the larval zebrafish brain (Figure 1A, Movie S1, and the Supplemental Experimental Procedures). In 5-day-old larval zebrafish, spiral fiber neurons are a group of approximately ten neurons located bilaterally in rhombomere 3, rostro-ventral of the M-cells. These neurons all have descending projections to the contralateral M-cell axon cap and do not appear to contact other targets [9]. We first asked whether spiral fiber neurons are capable of sensing stimuli that are classically used to elicit M-cell-dependent escapes (Figure 1B). In paralyzed animals embedded in agarose, we monitored calcium dynamics in spiral fiber neurons

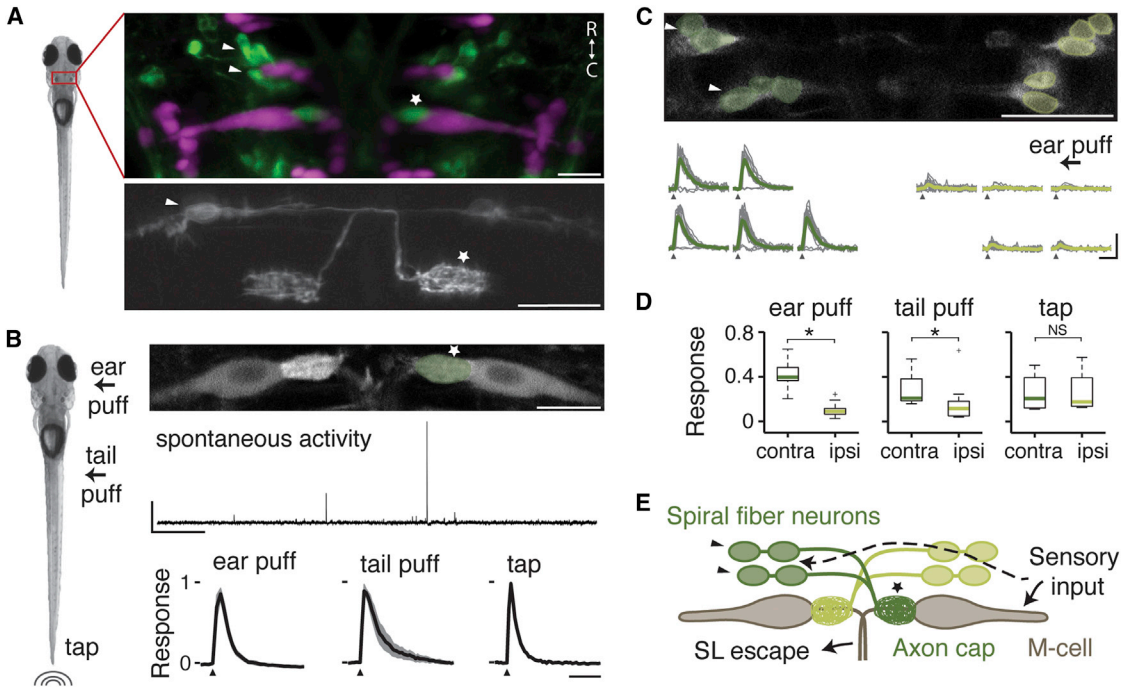


**Figure 1. Spiral Fiber Neurons Respond to Aversive Stimuli**

(A) Left: 5-day-old zebrafish larvae. Top: *Tg(–6.7FRhcrtR:gal4VP16)*; *Tg(UAS:GCaMP5)* labels spiral fiber neurons (arrowhead) among other neurons. The M-cell and other reticulospinal neurons are labeled with tetramethylrhodamine dextran by reticulospinal backfill. Spiral fiber neuron cell bodies are located in rhombomere 3 in two rostro-caudal (R↔C) clusters, approximately 25–40 μm rostral, 5–15 μm lateral, and 0–20 μm ventral of the axon cap (star). They all have axons descending contralaterally into the axon cap of the M-cell. Bottom: transient expression of membrane-targeted GFP (*UAS:GAP43-GFP*) in *Tg(–6.7FRhcrtR:gal4VP16)* labels two spiral fiber neurons on the left and one spiral fiber neuron on the right that project to the contralateral M-cell axon cap.

(B) Left: three different stimuli were delivered to paralyzed zebrafish larvae—water puffs directed at the right ear, water puffs directed at the right side of the tail, and non-directional taps delivered onto the dish holding the fish. Top: projection of two-photon image stack showing M-cells and spiral fiber neuron axon terminals labeled with the calcium indicator *Tg(UAS:GCaMP-HS)* driven by *Et(fos:Gal4-VP16)s1181t* and *Tg(–6.7FRhcrtR:gal4VP16)*, respectively. middle: Typical spontaneous activity in the spiral fiber neuron axon terminals. Scale bars represent 5 min horizontally and1 Δf/f vertically. Bottom: mean response amplitude in the right spiral fiber neuron axon terminals for different stimuli: ear puffs (n = 7, left), tail puffs (n = 5, center), and taps (n = 6, right). For each fish, the change in fluorescence (Δf/f) from trials in which the axon cap was active was normalized to the maximum Δf/f across trials and then averaged. The black line is the mean across fish with the SEM shaded. Stimulus delivery is indicated by an arrowhead. The horizontal scale bar represents 2 s.

(C) Top: single recording plane showing spiral fiber neuron somata in *Tg(–6.7FRhcrtR:gal4VP16)*; *Tg(UAS:GCaMP-HS)*. Bottom: mean Δf/f across trials in green and individual trials in gray for spiral fiber neuron somata from the top panel located on the left (dark green) and on the right (light green) responding to a water puff delivered to the right ear (arrow). Contralateral spiral fiber neurons respond to the stimulus, but ipsilateral spiral fiber neurons do not. Traces in which spiral fiber neurons on the left do not respond correspond to the same trials. Note that while caudal neurons seem to respond before rostral neurons, this is an artifact of the delay introduced by two-photon line scanning. Scale bars represent 2 s horizontally and 2 Δf/f vertically.

(D) Boxplot showing the normalized response of spiral fiber neurons across fish. Response was defined as the area under the Δf/f curve over a 1.5 s response window. This was normalized for each cell to the maximum response observed in a given experiment, and then cells located on the contralateral and ipsilateral side with respect to the stimulus were averaged. Green lines are the medians across fish, box edges are the 25$^{th}$ and 75$^{th}$ percentiles, the whiskers extend to the most extreme data points not considered outliers, and crosses are outliers. The following stimuli were delivered: ear puffs (left; n = 10 fish, $p = 2.5 \times 10^{-4}$), tail puffs (center; n = 10, p = 0.02), and taps (right; n = 4, p = 0.89). *$p < 0.05$; NS, not significant by Wilcoxon rank-sum test.

(E) Model showing the M-cells receiving ipsilateral sensory input, which includes auditory/vestibular afferents onto the lateral dendrite. Our results suggest that spiral fiber neuron somata receive similar sensory information from the contralateral side.

Pictures are oriented rostral up. Scale bars represent 20 μm. Arrows point to spiral fiber neuron somata, and a star indicates spiral fiber neuron terminals at the M-cell axon cap. Contra, contralateral; ipsi, ipsilateral; SL, short latency. See also Figure S1 and Movie S1.

labeled with the genetically encoded calcium indicator GCaMP-HS [14] by two-photon microscopy. We first assessed activity in the spiral fiber neuron axon terminals that wrap around the M-cell axon hillock. We observed irregular and infrequent spontaneous activity in spiral fiber neurons, at a rate of about one calcium event per minute (Figure 1B). We then stimulated the animals with three different stimuli: two tactile stimuli consisting of short water pulses delivered either to the otic vesicle (which develops into the ear) [7] or to the tail [6, 15], and a third stimulus that was a primarily auditory/vibrational stimulus consisting of an abrupt tap on the dish holding the animal (similar to [8]). We observed that all three types of stimuli elicited robust responses in the spiral fiber neuron axon terminals (Figure 1B). These responses were independent of M-cell activity: after bilateral M-cell ablations, spiral fiber neurons continued to respond to the tap stimulus with comparable amplitude (Figure S1). Thus, spiral fiber neurons encode a range of sensory information.

M-cells respond to stimuli arriving ipsilaterally on their dendrites, but individual spiral fiber neurons cross the midline and

project to the contralateral M-cell. We thus asked whether the responses of spiral fiber neurons were lateralized accordingly. Consistent with their contralateral projections, we observed that spiral fiber neuron somata were strongly activated by ear and tail stimuli delivered on the contralateral side (Figures 1C and 1D). Ipsilateral spiral fiber neurons also responded but more weakly (ear stimuli: $n = 10$ fish, $p < 0.05$, contralateral versus ipsilateral; tail stimuli: $n = 10$, $p < 0.05$; Wilcoxon rank-sum test), an effect most likely due to directional stimuli also being capable of stimulating the opposite side of the skin to a lesser extent. Responses to the non-directional tap stimulus, on the other hand, were not lateralized (Figure 1D, $n = 4$, $p > 0.05$). These results indicate that spiral fiber neurons receive contralateral sensory input and that as they cross the midline, the laterality of sensory information is preserved across M-cell inputs (Figure 1E).

## Spiral Fiber Neuron Ablations Largely Abolish M-Cell-Dependent Short-Latency Escapes

To investigate whether spiral fiber neurons affect the escape behavior, we built an apparatus designed to elicit and quantify escapes in response to an aversive stimulus. 5- to 7-day old fish were embedded in agarose, and their tails were freed. A mechanical tapper hit the plate onto which the fish was placed, in a similar manner to the tap stimulus used for calcium imaging experiments. By imaging at 1,000 Hz, we were able to reconstruct the curvature of the tail as a function of time and to measure the direction, angle, and latency of the response (Figure 2A). The tap stimulus elicited responses with 100% probability ($n = 50$ larvae). The vast majority (99.7%) of these responses were escapes, with latencies ranging from 5–25 ms (9.9 ± 0.19 ms, mean ± SEM). Characteristic escapes consisted of a sharp-angle C-bend of the tail (>60°), followed by a counter turn in the opposite direction and subsequent swimming lasting hundreds of milliseconds (Figure 2A). In accordance with previous findings [8, 16], we classified escapes as either short latency (≦12 ms) or long latency (13–25 ms). Larvae produced short-latency escapes with a high probability (92% ± 1.4%), whereas long-latency escapes were observed infrequently (8.2% ± 1.4%). Responses with latencies above 25 ms (0.26% ± 0.19%) corresponded to other types of movements, such as swims and turns. To uncover the types of sensory systems activated by the tap stimulus, we measured tap responses in fish with non-functional hair cells (*mariner* mutants [17]) and in fish in which the lateral line was ablated by neomycin treatment [18]. Our results indicate that short-latency escapes, but not long-latency escapes, are primarily mediated by the ear, whereas the lateral line does not play a role (Figure S2). Thus, tap stimuli engage several sensory systems, including the ear.

To analyze the respective contributions of the M-cell and spiral fiber neurons to the escape behavior, we compared the response to taps of larvae before and after three ablation conditions: M-cells (Figure 2B), spiral fiber neurons (Figure 2E), or ablation of other neurons in the area as a control (Figure 2H). Targeted ablations were carried out using a pulsed infrared laser as described previously [19]. Previous studies have shown that short-latency escapes in response to auditory stimuli require the M-cells, but tactile stimuli only partially depend on the M-cells [6, 7, 15, 20]. Two sets of segmental homologs are thought to elicit escapes of longer latency when the M-cell does not fire [6, 7, 21]. Thus, due to the multisensory nature of our stimulus, we expected the M-cells to be partially required for short-latency escapes. Indeed, we found that after M-cell ablations, the number of short-latency escapes performed decreased in favor of long-latency escapes ($n = 14$ fish; Figure 2C). The mean probability of short-latency escapes decreased on average 1.8-fold, and long-latency escapes increased 3-fold ($p < 0.05$, Wilcoxon signed-rank test; Figure 2D). Spiral fiber neuron ablations had a similar effect: after ablations, the majority of escapes observed were long latency (Figure 2F). Short-latency escapes were reduced by 6-fold, and long-latency escapes increased 8.1-fold ($n = 13$, $p < 0.05$; Figure 2G). Control ablations did not induce a change in the escape latency profile (Figure 2I) or probability of escapes ($n = 23$, $p > 0.05$; Figure 2J). The overall probability of response was not affected by any of the ablation procedures (Figures 2D, 2G, and 2J).

To compare the effect of ablation across groups, we evaluated the change in short-latency escape probability after ablations. The effects of M-cell and spiral fiber neuron ablations were significantly different from controls ($p < 0.05$, Wilcoxon rank-sum test; Figure 2K). A fraction of M-cell ablations did not produce a strong effect, most likely due to compensatory escape pathways. Nevertheless, the effects of M-cell and spiral fiber neuron ablations were not statistically distinguishable from each other ($p > 0.05$). Taken together, these experiments show that the phenotype after ablation of spiral fiber neurons is similar to that of ablation of M-cells, indicating that spiral fiber neurons play an essential role in M-cell-mediated escapes.

## Spiral Fiber Neurons Are Involved in the Laterality of M-Cell-Mediated Escapes

M-cells provide excitation to the contralateral side of the spinal network, resulting in contralateral tail bends. Due to inhibition [22, 23], only one of the two M-cells elicits an escape response at any one time. In accordance with this circuit design, previous studies have shown that after unilateral M-cell ablation, the probability of contralateral short-latency escape is decreased, with a concomitant increase in ipsilateral short-latency escapes [8]. Since spiral fiber neurons project to one M-cell only, we asked whether they also affect the escape behavior in a lateralized manner. To test this, we compared the effect of unilateral M-cell (Figure 3B) and spiral fiber neuron (Figure 3C) ablations on the directionality of the escape behavior in response to non-directional tap stimuli (Figure 3A). We expected that following the anatomy of the circuit, ablation of one M-cell or its contralateral spiral fiber neurons would bias escapes toward the ipsilateral and contralateral side with respect to the ablated somata, respectively (Figure 3E). We found that the overall frequency of short-latency escapes did not change after M-cell ablations (Figure 3D). However, as expected, unilateral M-cell ablations biased escapes toward one side (Figure 3F). Regardless of the original directional preference of individual fish before ablations, in all cases short-latency escapes contralateral to the ablated M-cell were virtually eliminated ($n = 11$, 35% ± 9.0% pre to 7.0% ± 3.6% post; Figure 3G). The directionality of the other, infrequent types of responses, such as long-latency escapes and swims, was not affected by the ablations (data not shown). Unilateral ablation of spiral fiber neurons had a similar effect as ablation of the

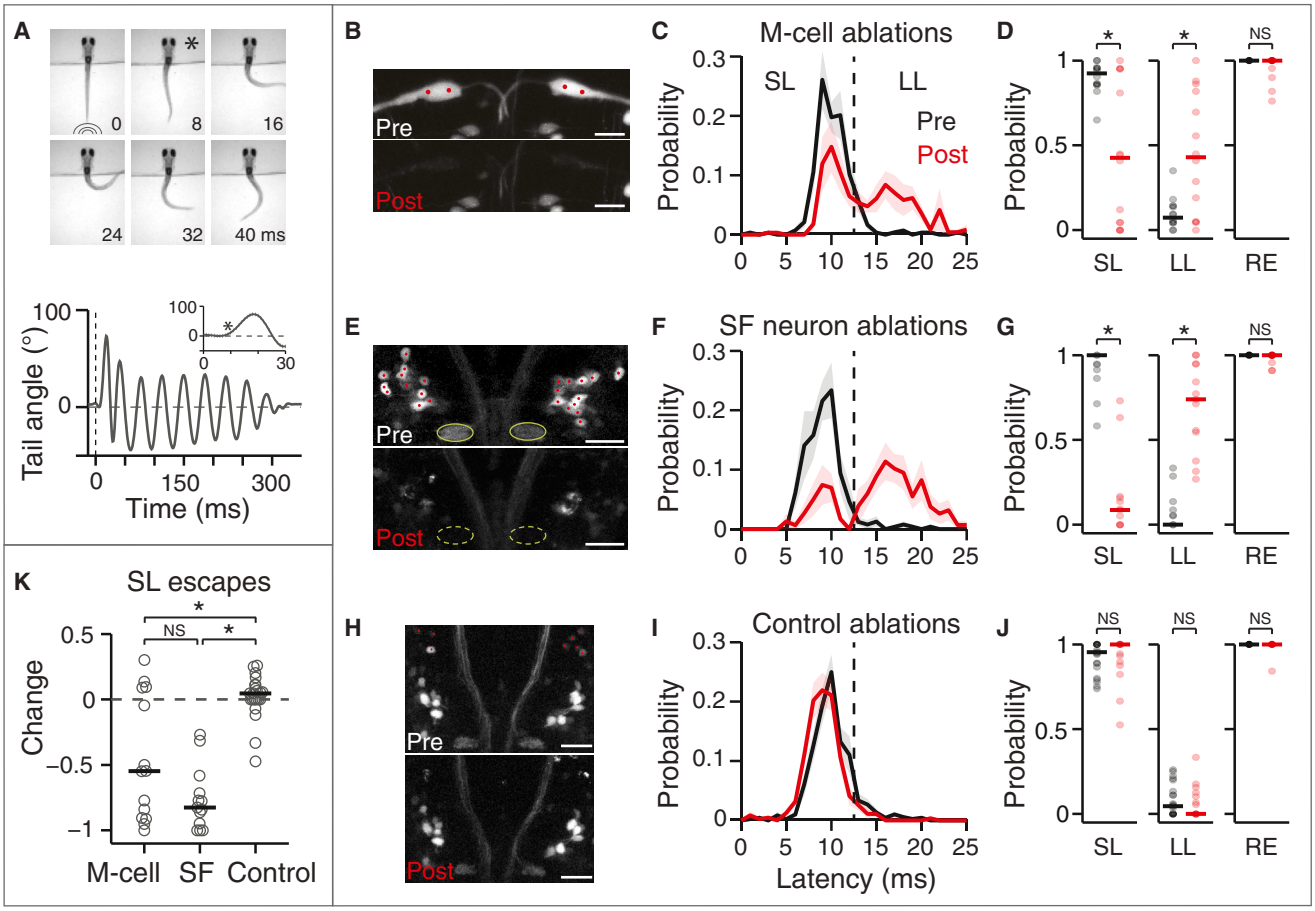


**Figure 2. Loss of M-Cells or Spiral Fiber Neurons Largely Abolish Short-Latency Escapes**

(A) Top: representative escape behavior of a head-embedded larval zebrafish responding to a tap stimulus. Images were recorded every millisecond, and here every eighth image is shown. The first image was taken at the time the tap stimulus hit the dish holding the larvae. The image marked with a star corresponds to the beginning of the escape response (8 ms latency). Bottom: representative smoothed tail trace showing the angle of the last tail segment with respect to the vertical in response to a tap. The escape behavior consists of a sharp-angle C-bend, followed by a counter turn in the opposite direction and subsequent swimming lasting hundreds of milliseconds. The dotted line shows the stimulus. The inset shows the first 300 ms after stimulus onset and the star indicates the start of the C-bend.

(B–J) Results of M-cell ablations (B–D; n = 14 fish), spiral fiber (SF) neuron ablations (E–G; n = 13), and control ablations (H–J; n = 23) on the escape behavior in response to taps.

(B, E, and H) Stack projections showing before (top) and immediately after (B) or 24 hr after (E and H) two-photon laser-mediated bilateral ablations (bottom). Shown are *Et(fos:Gal4-VP16)s1181t*; *Tg(UAS:GCaMP-HS)* (B) and *Tg(–6.7FRhcrtR:gal4VP16); Tg(UAS-E1b:Kaede)* (E and H). Red dots mark the cells or location within the M-cell that were targeted for ablation. Green ovals in (E) mark the axon caps, which are no longer apparent 24 hr after ablations. High-fluorescence cell debris can be observed in the post images.

(C, F, and I) Escape probability as a function of latency of all escapes performed, mean ± SEM, before (black) and after (red) ablations. The dotted line at 13 ms demarcates short-latency (≦12 ms) and long-latency (13–25 ms) escapes.

(D, G, and J) Probabilities of different types of responses as a function of all trials before (black) and after (red) ablations. Individual fish are displayed as semi-transparent dots, and horizontal bars are the medians. Left, SL escapes; middle, LL escapes; right, overall responses. M-cell: p = 0.013 pre versus post (SL), 0.016 (LL), and 0.125 (RE); spiral fiber neuron: $p = 2.4 \times 10^{-4}$, $p = 2.4 \times 10^{-4}$, and p = 0.25; control: p = 0.28, p = 0.20, and p = 1; Wilcoxon signed-rank test.

(K) Change in SL escape probability as a function of all trials (post – pre) based on the SL data plotted in (D), (G), and (J). Gray circles, individual fish; black line, median. M-cell versus spiral fiber neurons, p = 0.11; M-cell versus control, p = 0.011; spiral fiber neurons versus control, $p = 1.6 \times 10^{-6}$; Wilcoxon rank-sum test.

*p < 0.05; NS, not significant. Pictures are oriented rostral up. Scale bars represent 20 μm. SF, spiral fiber; LS, short latency; LL, long latency; RE, overall response. See also Figure S2.

M-cell they project to (Figure 3F). The percentage of short-latency escapes contralateral to the ablated spiral fiber neuron somata increased from 44% ± 6.4% to 91% ± 4.1% (n = 17; Figure 3G), whereas the overall fast-escape escape probability remained unchanged (Figure 3D). The laterality bias after M-cell or spiral fiber neuron ablation was not statistically distinguishable (p > 0.05). These experiments support the requirement of spiral fiber neurons for the normal functioning of their target M-cell.

## Spiral Fiber Neuron Activation Enhances the Probability of M-Cell-Mediated Escapes

Our results demonstrate that spiral fiber neurons are an essential excitatory input in the M-cell circuit. We next asked whether

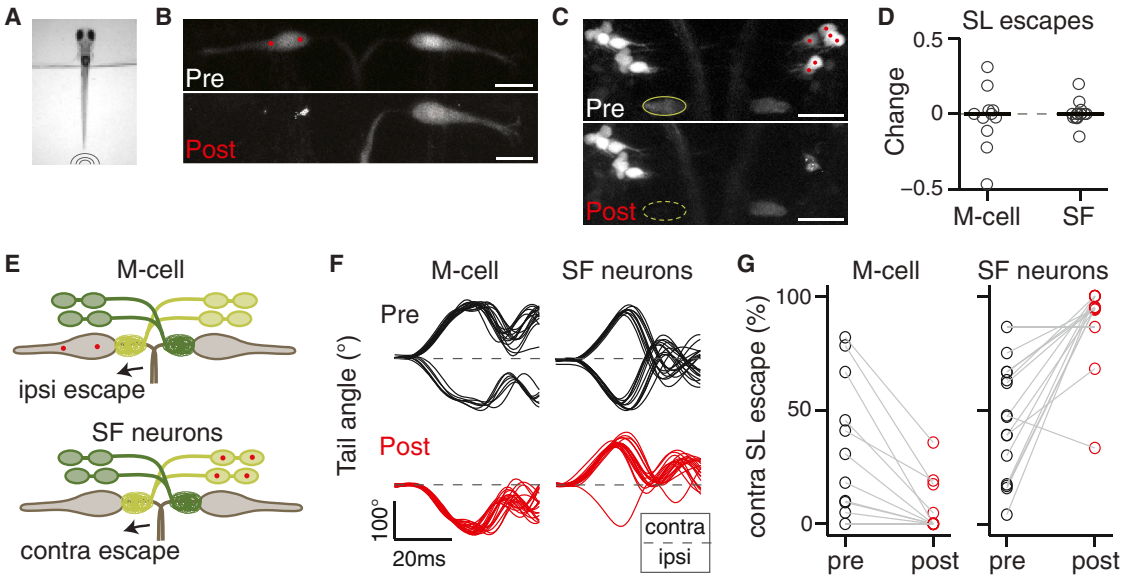


**Figure 3. Spiral Fiber Neurons Are Necessary for Lateralized M-Cell-Mediated Escapes**

(A) Tail-free larvae are presented with a non-directional tap stimulus as in Figure 2.

(B) Projection of two-photon image stack showing M-cells before (top) and 24 hr after (bottom) ablation of the M-cell on the left in *Et(fos:Gal4-VP16)s1181t; Tg(UAS-E1b:Kaede)*.

(C) Projection of two-photon image stack showing spiral fiber neurons before (top) and 24 hr after (bottom) ablation of spiral fiber neuron somata located on the right in *Tg(–6.7FRhcrtR:gal4VP16); Tg(UAS-E1b:Kaede)*. The axon cap (green oval) contralateral to the targeted spiral fiber neurons is no longer apparent 24 hr after ablations.

(D) Normalized change in short-latency (SL) escape probability as a function of all trials (post – pre). Gray circles, individual fish; black line, median. Left: M-cell ablation (n = 11). Right: spiral fiber neuron ablations (n = 17). The probability change is not significantly different from 0 in either condition (p = 0.67 and p = 0.98, respectively; Wilcoxon signed-rank test).

(E) Model showing that when M-cells or spiral fiber neurons are ablated unilaterally, escapes in response to taps become strongly biased toward one direction: ipsilateral to the ablated M-cell or contralateral to the ablated spiral fiber neurons.

(F) Example tail traces for a fish before (top plots; black) and after (bottom plots; red) ablation of the left M-cell (left plots) and a fish before and after ablations of spiral fiber neuron somata on the right (right plots). The directionality of the initial tail bend is expressed as ipsilateral or contralateral with respect to the ablated soma(ta). Traces begin at the time of tap delivery.

(G) Probability of contralateral SL escapes as a function of all SL escapes of either direction. Left: M-cell ablation. Right: spiral fiber neuron ablation. Escapes shift toward the ipsilateral side for M-cell ablation and to the contralateral side for spiral fiber neuron ablations. The laterality bias after M-cell or spiral fiber neuron ablation was not statistically distinguishable (p = 0.45, Wilcoxon rank-sum test).

Scale bars: 20 μm. Pictures are oriented rostral up. SF, spiral fiber; LS, short latency; contra, contralateral; ipsi, ipsilateral.

activating the spiral fiber neurons could decrease the threshold for M-cell-mediated escapes. To test this hypothesis, we used *Tg(14xUAS-E1b:hChR2(H134R)-EYFP)* to express channelrhodopsin2 (ChR2) in neurons labeled in *Tg(–6.7FRhcrtR:gal4VP16)*. We measured larval responsiveness to low-intensity taps alone or paired with blue light. ChR2 excitation light was delivered via a blue laser beam focused on the fish's head 20–60 ms before the tap occurred and for a total of 100 ms (Figure 4A). We observed a strong enhancement of short-latency, M-cell-mediated escapes in ChR2$^+$ fish when the weak taps were paired with blue light (4.4-fold enhancement; $p < 0.05$, Wilcoxon signed-rank test), but not in controls lacking ChR2 (Figure 4B). In addition to modulating the probability of short-latency escapes, we reasoned that the excitatory effect of spiral fiber neurons on the M-cell might decrease escape latency. Indeed, short-latency escapes in response to taps paired with light occurred on average 0.95 ms earlier than those in response to taps alone in ChR2$^+$ fish ($p < 0.05$). Latency was not affected in ChR2$^-$ controls (Figure 4C). The probability of long-latency escapes was also moderately enhanced by pairing taps with blue light in ChR2$^+$ fish only (2.1-fold mean increase), most likely due to unspecific ChR2-mediated effects. The latency of these escapes was not affected (Figures S3A and S3B).

To determine whether the ChR2-mediated enhancement of short-latency escapes was dependent on spiral fiber neurons, we tested behavior after spiral fiber neuron ablations. Short-latency escapes in response to taps alone were nearly abolished after spiral fiber neuron ablations, confirming our earlier ablation results. Crucially, pairing taps with blue light did not increase the probability of these escapes (Figure 4D). Our results suggest that spiral fiber neurons are necessary for the ChR2-mediated enhancement of M-cell-mediated escapes.

We next asked whether excitation of spiral fiber neurons alone could evoke escape behaviors. In half of the larvae (11/22), a 100-ms blue light pulse gave rise to escapes with a probability above 10% (Figure 4E). Spiral fiber neuron ablations eliminated these escapes in all but one larva, where lesions may have been incomplete. Optically induced escapes were kinematically similar to those induced by taps, but the angle of the initial C-bend was lower (Figures S3C and S3D), in agreement with

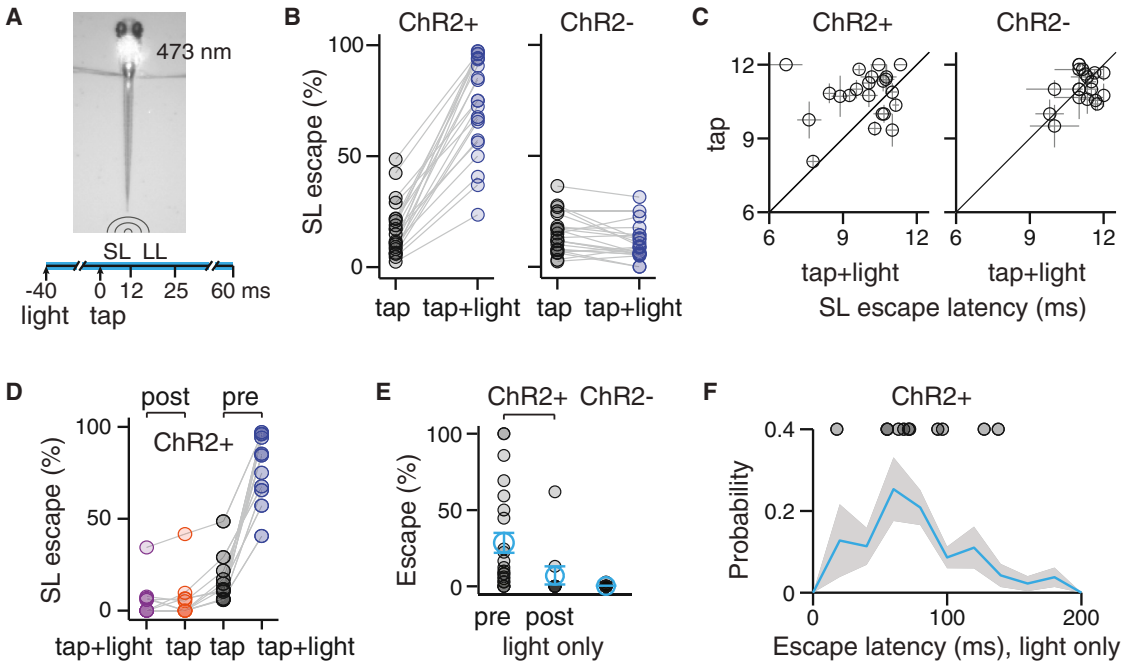


**Figure 4. Activation of Spiral Fiber Neurons Enhances the Probability of M-Cell-Mediated Escapes**

(A) 473-nm blue light is shone on the hindbrain of *Tg(–6.7FRhcrtR:gal4VP16); Tg(14xUAS-E1b:hChR2(H134R)-EYFP)* larvae using a focused laser beam for a total of 100 ms. 20–60 ms after the onset of the light, a low-intensity tap is delivered, and tail movements are scored for short-latency (SL) or long-latency (LL) escapes.

(B) Percentage of SL escapes for individual fish in response to taps alone (black circles) and taps paired with blue light (blue circles). Left: $ChR2^+$ fish (n = 22; 17% ± 4.9% tap, 73.4% ± 4.7% tap + light, mean ± SEM, corresponding to a 4.4-fold enhancement of SL escapes with blue light; $p = 4.0 \times 10^{-5}$). Right: $ChR2^-$ controls (n = 22; 15% ± 1.9% tap, 11% ± 1.7% tap + light, corresponding to a 1.4-fold decrease of SL escapes with blue light; p = 0.01, Wilcoxon signed-rank test).

(C) SL escape latency in milliseconds in response to taps (y axis) or taps paired with blue light (x axis) for individual fish tested (black circles). Left: $ChR2^+$ fish (n = 22; 11 ± 0.22 ms tap, 9.9 ± 0.27 ms tap + light, mean ± SEM; p = 0.01). Right: $ChR2^-$ fish (n = 22; 11 ± 0.14 ms tap, 11 ± 0.13 ms ms tap + light; p = 0.72, Wilcoxon signed-rank test).

(D) Percentage of SL escapes in response to taps or taps paired with light before (pre) or after (post) bilateral spiral fiber neuron ablations. (n = 11 $ChR^+$ larvae; pre: 17% ± 3.7% tap, 78 ± 5.4% tap + light, mean ± SEM, corresponding to a 4.7-fold enhancement; $p = 9.8 \times 10^{-4}$; post: 6.3% ± 3.5% tap, 5.6 ± 2.9% tap + light, p = 0.58; Wilcoxon signed-rank test). Data in the pre condition are a subset of the data in (B).

(E) Percentage of escapes for individual fish (black circles, mean ± SEM in blue) in response to blue light alone (in the absence of taps). $ChR2^+$ fish before (pre; n = 22) and after (post; n = 11) spiral fiber neuron ablations. $ChR2^-$ fish, n = 22.

(F) Distribution of escape latencies in $ChR2^+$ fish after the onset of a 100-ms blue light pulse (blue line ± shaded SEM; n = 185 escapes, n = 11 fish). Circles represent the mean of escape latencies for larvae displaying >10% probability of escapes (see "pre" in E; n = 11). Note: to ensure that escapes to blue light alone could be disambiguated with escapes in response to taps paired with light, larvae that responded to blue light alone with mean escapes latencies <70 ms were tested with a 20-ms delay between taps and blue light; otherwise, 40- or 60-ms delays were used (see A). See also the Supplemental Experimental Procedures. ChR2, channelrhodopsin 2; LS, short latency; LL, long latency. See also Figure S3.

reports that electrical stimulation of the M-cell alone gives rise to less effective escapes [24]. The latency from onset of blue light to behavior was long and variable (70 ± 30 ms, mean ± SD; Figure 4F), which is not unusual for ChR2-mediated behavior [25–27] (but see [28]). The effectiveness of blue light correlated with escape latencies across fish (Figures S3E–S3G) and most likely reflects ChR2 expression levels. Together, our optogenetic results indicate that exciting the spiral fiber neurons potentiates M-cell-mediated behavior.

## DISCUSSION

Our study unveils a functional pathway by which sensory information is indirectly conveyed to the escape circuit: spiral fiber neurons respond to aversive cues and excite the M-cell at the axon cap. We provide three lines of evidence that support the notion that spiral fiber neurons are essential for M-cell-mediated escapes: (1) like M-cell ablations, bilateral spiral fiber neuron ablations nearly abolish short-latency escapes; (2) ablation of spiral fiber neurons unilaterally shifts the directionality of escapes; and (3) optical activation of spiral fiber neurons enhances M-cell-mediated escapes in response to subthreshold stimuli. In the following sections, we relate our data to previous electrophysiological studies of the M-cell, discuss the utility of a spatially and temporally distinct convergent pathway, and describe how convergent pathways may be an important motif in neural circuits.

### Spiral Fiber Neuron Input Is Integrated with Dendritic Afferents at the M-Cell Axon Hillock

Previous electrophysiological recordings in the goldfish have identified an input of unknown origin onto the M-cell [29]. Our

findings suggest that this input has the characteristics of spiral fiber neuron excitation. In response to natural sounds, M-cell activity is composed of spatially and temporally distinct components: fast repetitive EPSPs are superimposed on an underlying slower depolarization [29]. Auditory/vestibular afferents making mixed electrical and chemical synapses on the M-cell lateral dendrites [30–32] are responsible for the fast component of the M-cell response and for part of the slower component [29]. The slower component also relies on an electrical and glutamatergic input near the soma [29], but the origin of this input is unknown. Spiral fiber neurons make both electrical and glutamatergic synapses close to the M-cell soma [9], and we find that they are active in response to sensory stimuli. This suggests that they are the origin of the secondary, slower component of the M-cell response, which was observed approximately 3 ms after the onset of the fast component. A 3-ms delay places this slower input within the M-cell's integration window: in response to auditory stimuli, initial depolarization in the goldfish M-cell occurs within 1 ms, but firing occurs from 3–12 ms [5, 33, 34]. Thus, in response to auditory/vibrational stimuli, excitatory inputs to the M-cell converge from two temporally and spatially distinct sources: distal sensory afferents provide rapid electrical and slower chemical input, and spiral fiber neurons provide a slow proximal input. Viral tracing experiments [35, 36] or other approaches are needed to identify the inputs of spiral fiber neurons.

To infer the site of integration of the dendritic and indirect inputs onto the M-cell, we recorded stimulus-elicited calcium activity in the M-cell soma before and after spiral fiber neuron ablations (Figure S4). We found that spiral fiber neuron ablations did not significantly affect calcium dynamics in the M-cell soma in response to taps, suggesting that dendritic inputs are responsible for the bulk of the somatic depolarization. Since spiral fiber neurons play a necessary role in M-cell-mediated motor output, these experiments argue that inputs from spiral fiber neurons and direct sensory afferents are integrated at the level of the M-cell axon hillock to elicit an escape response (see the Supplemental Results and Discussion associated with Figure S4). Electrophysiological recordings of the M-cell axon and soma and specific activation of spiral fiber neurons are needed to explicitly determine the nature of this spatiotemporal integration.

## Spiral Fiber Neurons Represent a Convergent Input that Enhances Circuit Robustness

Short-latency escapes, which are triggered by a single firing event in the M-cell, are vital to avoid predation but should be restricted to legitimate threats. Therefore, the M-cell must be reliably activated when necessary and otherwise be appropriately gated. The robust activation of the M-cell is faced with three hurdles: first, due to a low input resistance, short time constant, and hyperpolarized membrane potential, the M-cell requires strong currents to reach firing threshold [37]; second, feed-forward interneurons inhibit the M-cell [38, 39]; and third, dendritic excitation is strongly attenuated by the time it reaches the soma due to passive cable properties (up to 4-fold in the adult goldfish M-cell [29]). By providing an excitatory drive directly at the axon hillock, the site of action potential generation [40], spiral fiber neurons solve the challenge of overcoming the M-cell's high activation barrier. An additional challenge in the circuit is to ensure that the M-cell is not activated by innocuous short-lived sounds. Spiral fiber neurons introduce a delay line that may prevent unnecessary firing of the M-cell: transient depolarization of the M-cell by dendritic afferents would end before the necessary spiral fiber neuron input arrives at the axon hillock, precluding integration of the two pathways and rendering brief sensory input ineffective. Thus, in the M-cell escape circuit, indirect proximal input provides a necessary excitatory drive undiminished by distance and can serve as a mechanism to filter noise. Experiments combining stimulation of the two pathways and recordings in the M-cell are needed to directly test these scenarios.

## Indirect Excitatory Pathways as a Circuit Motif

The spiral fiber neuron input is the first example of a necessary indirect pathway in a startle circuit. A diverse set of other circuits present anatomical similarities, where multiple, sometimes temporally and spatially segregated excitatory pathways converge. The interaction of inputs in these networks is poised to enhance the controllability and flexibility of the system and may provide additional opportunities for modulation. A first example is the crayfish escape network, in which tactile afferents project to command neurons and also to excitatory interneurons that then feed forward to the command neurons. The amplitude of excitation elicited by the interneurons is larger than the excitation coming from direct tactile afferents [41], suggesting that like spiral fiber neurons in the M-cell circuit, these crayfish interneurons might be essential for producing escapes. Another example is the mammalian hippocampus where CA1 pyramidal neurons receive sensory information via a direct and an indirect pathway. One path projects monosynaptically onto the neurons' distal dendrites but has a weak influence over somatic voltage. A slower trisynaptic pathway projecting to the proximal dendrites provides a stronger input [42]. Thus, similarly to spiral fiber neuron inputs in the M-cell circuit, the indirect pathway to CA1 introduces a powerful delay line that is more proximal. These examples of comparable circuitry in invertebrates and mammals suggest that the necessity of convergent excitatory pathways might be a general motif of neural circuits.

## SUPPLEMENTAL INFORMATION

Supplemental Information includes Supplemental Results and Discussion, Supplemental Experimental Procedures, four figures, and one movie and can be found with this article online at http://dx.doi.org/10.1016/j.cub.2015.04.025.

## AUTHOR CONTRIBUTIONS

A.M.B.L., D.S. and A.F.S. conceived the study. D.S. generated the *Tg(–6.7FRhcrtR:gal4VP16)* line. A.M.B.L. collected the data. A.M.B.L. analyzed the data with the guidance of D.S. and discussions with all authors. A.M.B.L. built the behavioral and ChR2 apparatus with help from D.N.R., D.S., M.H., C.L.W., and R.P. and wrote the software with D.N.R. and M.H. D.N.R. and J.M.L. built the two-photon calcium imaging apparatus. O.R. generated Movie S1. A.M.B.L. and A.F.S. wrote the manuscript with contributions from D.S., M.H., R.P., O.R., and F.E.

## ACKNOWLEDGMENTS

We thank Adam Douglass and Jared Wortzman for generating the *Tg(UAS:GCaMP5)* fish; Koichi Kawakami for the *Tg(UAS:GCaMP-HS)* line; Herwig Baier for the *Et(fos:Gal4-VP16)s1181t* line; Joel Greenwood and Edward Soucy for technical support with the behavioral apparatus; Steve Zimmerman, Karen

Hurley, and Jessica Miller for fish care; and Misha Ahrens, Elizabeth Carroll, Timothy Dunn, Joseph Fetcho, Minoru Koyama, Florian Merkle, Iris Odstril, Yu-chin Pan, Carlos Pantoja, Constance Richter, Kristen Severi, and additional members of the F.E. and A.F.S. labs for many helpful discussions. A.M.B.L. was supported by a Theodore H. Ashford Graduate Fellowship in the Sciences, an NSF Graduate Research Fellowship, and NIH T32HL007901. D.S. was supported by a Helen Hay Whitney Postdoctoral Fellowship and NIDCD K99DC012775. M.H. was supported by an EMBO Long-Term Postdoctoral Fellowship (ALTF 1056-10) and a postdoctoral fellowship by the Jane Coffin Childs Fund for Biomedical Research. O.R. was supported by an HFSP Long-Term Fellowship (LT000772/2012). C.L.W. was supported by the Agency for Science, Technology and Research, Singapore. Research was supported by NIH grant R01HL109525 awarded to A.F.S.

Received: June 17, 2014
Revised: March 9, 2015
Accepted: April 14, 2015
Published: May 7, 2015

## REFERENCES

1. Zottoli, S.J., and Faber, D.S. (2000). The Mauthner cell: what has it taught us? Neuroscientist *6*, 26–38.
2. Eaton, R.C., Lee, R.K., and Foreman, M.B. (2001). The Mauthner cell and other identified neurons of the brainstem escape network of fish. Prog. Neurobiol. *63*, 467–485.
3. Korn, H., and Faber, D.S. (2005). The Mauthner cell half a century later: a neurobiological model for decision-making? Neuron *47*, 13–28.
4. Pfaff, D.W., Martin, E.M., and Faber, D. (2012). Origins of arousal: roles for medullary reticular neurons. Trends Neurosci. *35*, 468–476.
5. Zottoli, S.J. (1977). Correlation of the startle reflex and Mauthner cell auditory responses in unrestrained goldfish. J. Exp. Biol. *66*, 243–254.
6. Liu, K.S., and Fetcho, J.R. (1999). Laser ablations reveal functional relationships of segmental hindbrain neurons in zebrafish. Neuron *23*, 325–335.
7. Kohashi, T., and Oda, Y. (2008). Initiation of Mauthner- or non-Mauthner-mediated fast escape evoked by different modes of sensory input. J. Neurosci. *28*, 10641–10653.
8. Burgess, H.A., and Granato, M. (2007). Sensorimotor gating in larval zebrafish. J. Neurosci. *27*, 4984–4994.
9. Koyama, M., Kinkhabwala, A., Satou, C., Higashijima, S., and Fetcho, J. (2011). Mapping a sensory-motor network onto a structural and functional ground plan in the hindbrain. Proc. Natl. Acad. Sci. USA *108*, 1170–1175.
10. Kimmel, C.B., Sessions, S.K., and Kimmel, R.J. (1981). Morphogenesis and synaptogenesis of the zebrafish Mauthner neuron. J. Comp. Neurol. *198*, 101–120.
11. Scott, J.W., Zottoli, S.J., Beatty, N.P., and Korn, H. (1994). Origin and function of spiral fibers projecting to the goldfish Mauthner cell. J. Comp. Neurol. *339*, 76–90.
12. Lorent, K., Liu, K.S., Fetcho, J.R., and Granato, M. (2001). The zebrafish space cadet gene controls axonal pathfinding of neurons that modulate fast turning movements. Development *128*, 2131–2142.
13. Gyda, M., Wolman, M., Lorent, K., and Granato, M. (2012). The tumor suppressor gene retinoblastoma-1 is required for retinotectal development and visual function in zebrafish. PLoS Genet. *8*, e1003106.
14. Muto, A., Ohkura, M., Kotani, T., Higashijima, S., Nakai, J., and Kawakami, K. (2011). Genetic visualization with an improved GCaMP calcium indicator reveals spatiotemporal activation of the spinal motor neurons in zebrafish. Proc. Natl. Acad. Sci. USA *108*, 5425–5430.
15. O'Malley, D.M., Kao, Y.-H., and Fetcho, J.R. (1996). Imaging the functional organization of zebrafish hindbrain segments during escape behaviors. Neuron *17*, 1145–1155.
16. Ikeda, H., Delargy, A.H., Yokogawa, T., Urban, J.M., Burgess, H.A., and Ono, F. (2013). Intrinsic properties of larval zebrafish neurons in ethanol. PLoS ONE *8*, e63318.
17. Ernest, S., Rauch, G.J., Haffter, P., Geisler, R., Petit, C., and Nicolson, T. (2000). Mariner is defective in myosin VIIA: a zebrafish model for human hereditary deafness. Hum. Mol. Genet. *9*, 2189–2196.
18. Harris, J.A., Cheng, A.G., Cunningham, L.L., MacDonald, G., Raible, D.W., and Rubel, E.W. (2003). Neomycin-induced hair cell death and rapid regeneration in the lateral line of zebrafish (Danio rerio). J. Assoc. Res. Otolaryngol. *4*, 219–234.
19. Bianco, I.H., Ma, L.-H., Schoppik, D., Robson, D.N., Orger, M.B., Beck, J.C., Li, J.M., Schier, A.F., Engert, F., and Baker, R. (2012). The tangential nucleus controls a gravito-inertial vestibulo-ocular reflex. Curr. Biol. *22*, 1285–1295.
20. Kohashi, T., Nakata, N., and Oda, Y. (2012). Effective sensory modality activating an escape triggering neuron switches during early development in zebrafish. J. Neurosci. *32*, 5810–5820.
21. Issa, F.A., O'Brien, G., Kettunen, P., Sagasti, A., Glanzman, D.L., and Papazian, D.M. (2011). Neural circuit activity in freely behaving zebrafish (Danio rerio). J. Exp. Biol. *214*, 1028–1038.
22. Satou, C., Kimura, Y., Kohashi, T., Horikawa, K., Takeda, H., Oda, Y., and Higashijima, S. (2009). Functional role of a specialized class of spinal commissural inhibitory neurons during fast escapes in zebrafish. J. Neurosci. *29*, 6780–6793.
23. Takahashi, M., Narushima, M., and Oda, Y. (2002). In vivo imaging of functional inhibitory networks on the mauthner cell of larval zebrafish. J. Neurosci. *22*, 3929–3938.
24. Nissanov, J., Eaton, R.C., and DiDomenico, R. (1990). The motor output of the Mauthner cell, a reticulospinal command neuron. Brain Res. *517*, 88–98.
25. Douglass, A.D., Kraves, S., Deisseroth, K., Schier, A.F., and Engert, F. (2008). Escape behavior elicited by single, channelrhodopsin-2-evoked spikes in zebrafish somatosensory neurons. Curr. Biol. *18*, 1133–1137.
26. Kubo, F., Hablitzel, B., Dal Maschio, M., Driever, W., Baier, H., and Arrenberg, A.B. (2014). Functional architecture of an optic flow-responsive area that drives horizontal eye movements in zebrafish. Neuron *81*, 1344–1359.
27. Thiele, T.R., Donovan, J.C., and Baier, H. (2014). Descending control of swim posture by a midbrain nucleus in zebrafish. Neuron *83*, 679–691.
28. Monesson-Olson, B.D., Browning-Kamins, J., Aziz-Bose, R., Kreines, F., and Trapani, J.G. (2014). Optical stimulation of zebrafish hair cells expressing channelrhodopsin-2. PLoS ONE *9*, e96641.
29. Szabo, T.M., Weiss, S.A., Faber, D.S., and Preuss, T. (2006). Representation of auditory signals in the M-cell: role of electrical synapses. J. Neurophysiol. *95*, 2617–2629.
30. Nakajima, Y. (1974). Fine structure of the synaptic endings on the Mauthner cell of the goldfish. J. Comp. Neurol. *156*, 379–402.
31. Tuttle, R., Masuko, S., and Nakajima, Y. (1986). Freeze-fracture study of the large myelinated club ending synapse on the goldfish Mauthner cell: special reference to the quantitative analysis of gap junctions. J. Comp. Neurol. *246*, 202–211.
32. Lin, J.W., and Faber, D.S. (1988). Synaptic transmission mediated by single club endings on the goldfish Mauthner cell. I. Characteristics of electrotonic and chemical postsynaptic potentials. J. Neurosci. *8*, 1302–1312.
33. Eaton, R., and Lavender, W. (1981). Identification of Mauthner-initiated response patterns in goldfish: evidence from simultaneous cinematography and electrophysiology. J. Comp. Physiol. *144*, 521–531.
34. Weiss, S.A., Zottoli, S.J., Do, S.C., Faber, D.S., and Preuss, T. (2006). Correlation of C-start behaviors with neural activity recorded from the hindbrain in free-swimming goldfish (Carassius auratus). J. Exp. Biol. *209*, 4788–4801.
35. Zhu, P., Narita, Y., Bundschuh, S.T., Fajardo, O., Schärer, Y.P., Chattopadhyaya, B., Bouldoires, E.A., Stepien, A.E., Deisseroth, K., Arber, S., et al. (2009). Optogenetic dissection of neuronal circuits in zebrafish using viral gene transfer and the Tet system. Front Neural Circuits *3*, 21.

 

36. Mundell, N.A., Beier, K.T., Pan, Y.A., Lapan, S.W., Göz Aytürk, D., Berezovskii, V.K., Wark, A.R., Drokhlyansky, E., Bielecki, J., Born, R.T., et al. (2015). Vesicular stomatitis virus enables gene transfer and transsynaptic tracing in a wide range of organisms. J. Comp. Neurol. Published online February 17, 2015. http://dx.doi.org/10.1002/cne.23761.

37. Curti, S., and Pereda, A.E. (2010). Functional specializations of primary auditory afferents on the Mauthner cells: interactions between membrane and synaptic properties. J. Physiol. Paris *104*, 203–214.

38. Zottoli, S.J., and Faber, D.S. (1980). An identifiable class of statoacoustic interneurons with bilateral projections in the goldfish medulla. Neuroscience *5*, 1287–1302.

39. Faber, D.S., Fetcho, J.R., and Korn, H. (1989). Neuronal networks underlying the escape response in goldfish. General implications for motor control. Ann. N Y Acad. Sci. *563*, 11–33.

40. Furshpan, E.J., and Furukawa, T. (1962). Intracellular and extracellular responses of the several regions of the Mauthner cell of the goldfish. J. Neurophysiol. *25*, 732–771.

41. Zucker, R.S. (1972). Crayfish escape behavior and central synapses. I. Neural circuit exciting lateral giant fiber. J. Neurophysiol. *35*, 599–620.

42. Dudman, J.T., Tsay, D., and Siegelbaum, S.A. (2007). A role for synaptic inputs at distal dendrites: instructive signals for hippocampal long-term plasticity. Neuron *56*, 866–879.